Information Fusion of Airborne radar and ESM for maneuvering target tracking system based on IMM-BLUE

Bao-bao Wang
Jiangsu Automation Research Institute
No.18, Sheng Hu Road, Lianyungang 222006
PEOPLE'S REPUBLIC OF CHINA
wangbaobao_zdh@126.com

Lian-zheng Zhang
Nanjing University of Science and Technology
No.200,Xiao Ling Wei Street, Nanjing 210094
PEOPLE'S REPUBLIC OF CHINA
baolovexiaer@163.com

Abstract: In order to make full use of measurement information provided by sensors on the aerial carriers and efficiently make maneuvering target tracking under complicated conditions, this paper studies tracking methods of joint maneuvering target by airborne radar and Electronic Support Measure (ESM). Based on Interacted Multiple Model-Blue Linear Unbiased Estimation (IMM-BLUE) algorithm, this paper well tracks maneuvering target by airborne radar-ESM data fusion and has designed target tracking algorithm for airborne radar in Doppler blind zone (DBZ) as well as proposes two tracking methods separately for measured value of data fitting amount in DBZ and single ESM. Simulation results show IMM-BLUE algorithm well advantages over Extended Kalman Filter (EKF) by far avoiding the defect of divergement from the latter. Compared with simulation results of single radar, the data fusion tracking of airborne radar and ESM further improves tracking accuracy. Performances of either curve-fitting method in DBZ or single ESM tracking prove validity of the two methods in this paper. Radar-ESM joint tracking technology discussed in this paper has solved the problems caused by sensor unicity and Doppler blind zone.

Key-Words: Maneuvering target tracking, IMM-BULE, Information Fusion, DBZ, Airborne Radar, ESM

1 Introduction

With an increasing maneuverability of various new weapons, data from a single sensor can never meet the tactical demands. Only by fully making use of info from the observation platform can effectively track targets under complicated circumstances. Airborne radar and ESM are two important sensors on aerial carriers. Single airborne radar is unable to meet target tracking demand and DBZ limits intelligence effectiveness of airborne radar while airborne radar-ESM joint tracking technology can solve above problems.

Nowadays, multi-sensor data fusion as one of the key tracking technologies has been applied in airborne tracking systems and airborne radar and ESM are two important sensors of aerial carriers. Scholars have made a great deal of research of data fusion of airborne radar and ESM. Reference [1] make comparative analysis of associated filtering algorithms between radar and ESM; Reference [2] discuss data compression in radar-ESM collaborative tracking; Reference [3] present radar-ESM intermittent algorithm, a polynomial time tracking based on measurement time inconsistency of radar and ESM. Some scholars make study of how to track effectively of targets in DBZ. Reference [4] propose BDPF (blind Doppler particle filtering) algorithm, which predicts target state by applying particle filtering algorithm into DBZ and shape associated tracking window with bounded particles, well tracking of constant speed target. Reference [5] propose particle filtering tracking algorithm jointly constrained by DBZ and ESM azimuth info, which realize target tracking in DBZ and present smaller error than that of DBZ info only. Reference [6] propose a temporary elimination method of route optimization based on Doppler target prediction by combing extended Kalman filter-treated target dot prediction with route optimization criteria of traditional adaptive-prediction.

This paper studies maneuvering target tracking algorithm based on aerial carriers while IMM-BLUE method fulfils data fusion of airborne radar and ESM, improving the tracking accuracy compared with the single radar tracking. This paper further studies the joint tracking technology of radar and ESM in DBZ, putting forward with two tracking methods separately for DBZ data and single ESM tracking which are both proved to be effective by simulation results.

2 IMM-BLUE principle

2.1 Target tracking model

IMM covers several filters, one model probability estimator, one interactive effector and one estimator commingler. Algorithm recursion each time concludes the following four steps[7, 8].

1) Interaction of state estimation

Suppose there are r models, then transition probability from model i to model j is P_{ij}. Let $\hat{X}_i(k|k)$ as state estimation of filter i at time k, $P_i(k|k)$ as the corresponding covariance matrix and $\mu_i(k)$ as probability of model i at time k, while $i, j = 1,2,...,r$, then inputs of r filters at $k+1$ by interactive computing are as follows:

$$\hat{X}_{oi}(k|k) = \sum_{i=1}^{r} \hat{X}_i(k|k)\mu_{i|j}(k|k) \quad (1)$$

$$P_{oi}(k|k) = \sum_{i=1}^{r}[P_i(k|k) + (\hat{X}_i(k|k) - X_{oi}(k|k)) (\hat{X}_i(k|k) - X_{oi}(k|k))^T]\mu_{i|j}(k|k) \quad (2)$$

Where

$$\mu_{i|j}(k|k) = \frac{1}{\bar{C}_i} P_{ij}\mu_i(k) \quad (3)$$

$$\bar{C}_i = \sum_{i=1}^{r} P_{ij}\mu_i(k) \quad (4)$$

2) Model conditional filtering

Filter output is carried out as $\hat{X}_i(k+1|k+1)$ and $P_i(k+1|k+1)$ when taking $\hat{X}_{oi}(k|k)$ and $P_{oi}(k|k)$ as input in i model of $(k+1)$.

3) Updating model probability

$$\mu_i(k+1) = \frac{1}{C}\Lambda_i(k+1)\bar{C}_i \quad (5)$$

Where

$$C = \sum_{i=1}^{r}\Lambda_i(k+1)\bar{C}_i \quad (6)$$

$$\Lambda_i(k+1) = \frac{\exp[-\frac{1}{2}(\nu_i^T(k+1))S_i^{-1}(k+1)\nu_i(k+1)]}{\sqrt{|2\pi S_i(k+1)|}} \quad (7)$$

Where

$$\nu_i(k+1) = Z(k+1) - H_i(k+1)\hat{X}_i(k+1|k) \quad (8)$$

$$S_i(k+1) = H_i(k+1)P_i(k+1|k)H_i^T(k+1) + R_i(k+1) \quad (9)$$

$Z(k+1)$ is the system measurement vector; $H_i(k+1)$ is measure matrix, $\nu_i(k+1)$ is measurement noise vector, $R_i(k+1)$ is the covariance of measurement noise.

4) Filter interacted output

$$\hat{X}(k+1|k+1) = \sum_{i=1}^{r}\hat{X}_i(k+1|k+1)\mu_i(k+1) \quad (10)$$

$$P(k+1|k+1) = \sum_{i=1}^{r}[(\hat{X}_i(k+1|k+1) - \hat{X}(k+1|k+1)) (\hat{X}_i(k+1|k+1) - \hat{X}(k+1|k+1))^T]\mu_i(k+1) + \sum_{i=1}^{r}P_i(k+1|k+1)\mu_i(k+1) \quad (11)$$

This paper selects CV model and Singer acceleration model interact [9,10]. State equation of the system is

$$X(k+1) = \Phi_i(k)X(k) + \Gamma_i(k)W_i(k) \quad (12)$$

Measurement equation is

$$Z(k) = HX(k) + V(k) \quad (13)$$

Where,

$X(k) = [x(k), y(k), z(k), \dot{x}(k), \dot{y}(k), \dot{z}(k), \ddot{x}(k), \ddot{y}(k), \ddot{z}(k)]^T$ serves as state vector of the system, including target's position, velocity and acceleration in X, Y and Z direction, respectively. Φ_1(k) is system state transition matrix of CV, Γ_1(k) is noise gain matrix of CV, W_1(k) is system process noise matrix of CV, Φ_2(k) is system state transition matrix of Singer, Γ_2(k) is noise gain matrix of Singer, W_2(k) is system process noise matrix of Singer, $Z(k)$ is the system measurement vector; H is measure matrix, $V(k)$ is measurement noise vector.

$$\Phi_1(k) = \begin{bmatrix} 1 & 0 & 0 & T & 0 & 0 & 0 & 0 & 0 \\ 0 & 1 & 0 & 0 & T & 0 & 0 & 0 & 0 \\ 0 & 0 & 1 & 0 & 0 & T & 0 & 0 & 0 \\ 0 & 0 & 0 & 1 & 0 & 0 & 0 & 0 & 0 \\ 0 & 0 & 0 & 0 & 1 & 0 & 0 & 0 & 0 \\ 0 & 0 & 0 & 0 & 0 & 1 & 0 & 0 & 0 \\ 0 & 0 & 0 & 0 & 0 & 0 & 0 & 0 & 0 \\ 0 & 0 & 0 & 0 & 0 & 0 & 0 & 0 & 0 \\ 0 & 0 & 0 & 0 & 0 & 0 & 0 & 0 & 0 \end{bmatrix} \quad (14)$$

$$\Phi_2(k) = \begin{bmatrix} 1 & 0 & 0 & T & 0 & 0 & \phi_{17} & 0 & 0 \\ 0 & 1 & 0 & 0 & T & 0 & 0 & \phi_{28} & 0 \\ 0 & 0 & 1 & 0 & 0 & T & 0 & 0 & \phi_{39} \\ 0 & 0 & 0 & 1 & 0 & 0 & \phi_{47} & 0 & 0 \\ 0 & 0 & 0 & 0 & 1 & 0 & 0 & \phi_{58} & 0 \\ 0 & 0 & 0 & 0 & 0 & 1 & 0 & 0 & \phi_{69} \\ 0 & 0 & 0 & 0 & 0 & 0 & e^{-\alpha_x T} & 0 & 0 \\ 0 & 0 & 0 & 0 & 0 & 0 & 0 & e^{-\alpha_y T} & 0 \\ 0 & 0 & 0 & 0 & 0 & 0 & 0 & 0 & e^{-\alpha_z T} \end{bmatrix} \quad (15)$$

Where

$$\phi_{17}=(\alpha_x T-1+e^{-\alpha_x T})/\alpha_x{}^2,\quad \phi_{28}=(\alpha_y T-1+e^{-\alpha_y T})/\alpha_y{}^2,$$
$$\phi_{39}=(\alpha_z T-1+e^{-\alpha_z T})/\alpha_z{}^2,\quad \phi_{47}=(1-e^{-\alpha_x T})/\alpha_x,$$
$$\phi_{58}=(1-e^{-\alpha_y T})/\alpha_y,\quad \phi_{69}=(1-e^{-\alpha_z T})/\alpha_z$$

$$\Gamma_1(k)=\begin{bmatrix}\Gamma_{11}\\ \Gamma_{12}\\ \Gamma_{13}\end{bmatrix} \tag{16}$$

$$\Gamma_2(k)=\begin{bmatrix}\Gamma_{21}\\ \Gamma_{22}\\ \Gamma_{23}\end{bmatrix} \tag{17}$$

Where

$$\Gamma_{11}=diag\left(\begin{bmatrix}T^2/2\\ T^2/2\\ T^2/2\end{bmatrix}\right)\qquad \Gamma_{12}=diag\left(\begin{bmatrix}T\\ T\\ T\end{bmatrix}\right)$$

$$\Gamma_{13}=diag\left(\begin{bmatrix}0\\ 0\\ 0\end{bmatrix}\right)$$

$$\Gamma_{21}=diag\left(\begin{bmatrix}\gamma_x\left[1-\alpha_x T-e^{-\alpha_x T}+(T^2\alpha_x{}^2/2)\right]/\alpha_x{}^3\\ \gamma_y\left[1-\alpha_y T-e^{-\alpha_y T}+(T^2\alpha_y{}^2/2)\right]/\alpha_y{}^3\\ \gamma_z\left[1-\alpha_z T-e^{-\alpha_z T}+(T^2\alpha_z{}^2/2)\right]/\alpha_z{}^3\end{bmatrix}\right)$$

$$\Gamma_{22}=diag\left(\begin{bmatrix}\gamma_x(\alpha_x T+e^{-\alpha_x T}-1)/\alpha_x{}^2\\ \gamma_y(\alpha T+e^{-\alpha_y T}-1)/\alpha_y{}^2\\ \gamma_z(\alpha T+e^{-\alpha_z T}-1)/\alpha_z{}^2\end{bmatrix}\right)$$

$$\Gamma_{23}=diag\left(\begin{bmatrix}\gamma_x(1-e^{-\alpha_x T})/\alpha_x\\ \gamma_y(1-e^{-\alpha_y T})/\alpha_y\\ \gamma_z(1-e^{-\alpha_z T})/\alpha_z\end{bmatrix}\right)$$

where, $\gamma_x=\gamma_y=\gamma_z=\gamma$, $\alpha_x=\alpha_y=\alpha_z=\alpha$ describes the first-order forming filter parameter of the attacking target's acceleration in the Cartesian coordinate. T is system measurement period.

$$H=\begin{bmatrix}1&0&0&0&0&0&0&0&0\\ 0&1&0&0&0&0&0&0&0\\ 0&0&1&0&0&0&0&0&0\end{bmatrix} \tag{18}$$

2.2 BLUE principle

If the BLUE estimate of given target at time $k-1$ is $\hat{x}_{k-1|k-1}$ and the responding error covariance matrix is $P_{k-1|k-1}$, then the motion state of the target at time k can be optimally estimated by the following recursive BLUE filters [11]:

$$\begin{cases}\hat{x}_{k|k-1}=F_{k-1}\hat{x}_{k-1|k-1}\\ \tilde{x}_{k|k-1}=X_k-\hat{x}_{k|k-1}\\ P_{k|k-1}=F_{k-1}P_{k-1|k-1}F^T{}_{k-1}+G_{k-1}Q_{k-1}G^T{}_{k-1}\end{cases} \tag{19}$$

$$\begin{cases}\hat{Z}_{k|k-1}=E^*[Z_k\mid Z^{k-1}]=[\hat{x}^c_{k|k-1},\hat{y}^c_{k|k-1},\hat{z}^c_{k|k-1}]^T\\ \tilde{Z}_{k|k-1}=Z_k-\hat{Z}_{k|k-1}\\ S_k=\mathrm{cov}[\tilde{Z}_{k|k-1}]\\ K_k=\mathrm{cov}[\tilde{x}_{k|k-1},\tilde{Z}_{k|k-1}]S_k^{-1}\end{cases} \tag{20}$$

$$\begin{cases}\hat{x}_{k|k}=\hat{x}_{k|k-1}+K_k\tilde{Z}_{k|k-1}\\ \tilde{x}_{k|k}=X_k-\hat{x}_{k|k}\\ P_{k|k}=\mathrm{cov}\left[\tilde{x}_{k|k}\right]=P_{k|k-1}-K_kS_kK_k^T\end{cases} \tag{21}$$

Therefore in formula (20), next measurement of Z_k is:

$$\begin{aligned}\hat{Z}_{k|k-1}&=[\hat{x}^c_{k|k-1},\hat{y}^c_{k|k-1},\hat{z}^c_{k|k-1}]^T\\ &=[\lambda_1\mu_1\hat{x}_{k|k-1}(1,1),\lambda_1\mu_1\hat{x}_{k|k-1}(2,1),\mu_1\hat{x}_{k|k-1}(3,1)]^T\end{aligned} \tag{22}$$

Where $\hat{x}_{k|k-1}(i,1), i=1,2,3$ stand for an element in line i , column1 of $\hat{x}_{k|k-1}$

In gain matrix K_k :

$$\begin{aligned}\mathrm{cov}[\tilde{x}_{k|k-1},\tilde{Z}_{k|k-1}]&=E[X_kZ_k^T]-E[\hat{x}_{k|k-1}\hat{z}^T_{k|k-1}]\\ &=\mu_1[\lambda_1P_{k|k-1}(\cdot,1),\lambda_1P_{k|k-1}(\cdot,2),P_{k|k-1}(\cdot,3)]\end{aligned} \tag{23}$$

While $P_{k|k-1}(\cdot,j), j=1,2,3$ represent column vectors composed by column j of $P_{k|k-1}$.

Innovative covariance matrix of S_k is:

$$S_k=\begin{bmatrix}S_{11}&S_{12}&S_{13}\\ S_{21}&S_{22}&S_{23}\\ S_{31}&S_{32}&S_{33}\end{bmatrix} \tag{24}$$

Where

$$\begin{aligned}S_{11}=&\lambda_2\mu_2P_{k|k-1}(1,1)+\lambda_3\mu_2P_{k|k-1}(2,2)+\lambda_2\mu_2\sigma_r^2E\left[\frac{x_k^2}{r_k^2}\right]\\ &+\lambda_3\mu_2\sigma_r^2E\left[\frac{y_k^2}{r_k^2}\right]+\lambda_2\mu_3E\left[\frac{x_k^2z_k^2}{(x_k^2+y_k^2)}\right]+\lambda_3\mu_3E\left[\frac{y_k^2z_k^2}{(x_k^2+y_k^2)}\right]\\ &+\lambda_2\mu_3\sigma_r^2E\left[\frac{x_k^2z_k^2}{r_k^2(x_k^2+y_k^2)}\right]+\lambda_3\mu_3\sigma_r^2E\left[\frac{y_k^2z_k^2}{r_k^2(x_k^2+y_k^2)}\right]\\ &+(\lambda_2\mu_2-\lambda_1^2\mu_1^2)E\left[\hat{x}^2_{k|k-1}\right]+\lambda_3\mu_2E\left[\hat{y}^2_{k|k-1}\right]\end{aligned}$$

$$
\begin{aligned}
S_{22} &= \lambda_2\mu_2 P_{k|k-1}(2,2) + \lambda_3\mu_2 P_{k|k-1}(1,1) + \lambda_2\mu_2\sigma_r^2 E\left[\frac{y_k^2}{r_k^2}\right] \\
&\quad + \lambda_3\mu_2\sigma_r^2 E\left[\frac{x_k^2}{r_k^2}\right] + \lambda_2\mu_3 E\left[\frac{y_k^2 z_k^2}{(x_k^2+y_k^2)}\right] + \lambda_3\mu_3 E\left[\frac{x_k^2 z_k^2}{(x_k^2+y_k^2)}\right] \\
&\quad + \lambda_2\mu_3\sigma_r^2 E\left[\frac{y_k^2 z_k^2}{r_k^2(x_k^2+y_k^2)}\right] + \lambda_3\mu_3\sigma_r^2 E\left[\frac{x_k^2 z_k^2}{r_k^2(x_k^2+y_k^2)}\right] \\
&\quad + (\lambda_2\mu_2 - \lambda_1^2\mu_1^2) E\left[\hat{y}_{k|k-1}^2\right] + \lambda_3\mu_2 E\left[\hat{x}_{k|k-1}^2\right] \\
S_{33} &= \mu_2 P_{k|k-1}(3,3) + \mu_3\left\{P_{k|k-1}(1,1) + P_{k|k-1}(2,2)\right\} \\
&\quad + \mu_2\sigma_r^2 E\left[\frac{z_k^2}{r_k^2}\right] + \mu_3\sigma_r^2 E\left[\frac{(x_k^2+y_k^2)}{r_k^2}\right] \\
&\quad + (\mu_2 - \mu_1^2) E\left[\hat{z}_{k|k-1}^2\right] + \mu_3 E\left[\hat{x}_{k|k-1}^2 + \hat{y}_{k|k-1}^2\right] \\
S_{12} &= \mu_2(\lambda_2 - \lambda_3) P_{k|k-1}(1,2) + \mu_2\sigma_r^2(\lambda_2 - \lambda_3) E\left[\frac{x_k y_k}{r_k^2}\right] \\
&\quad + \mu_3(\lambda_2 - \lambda_3) E\left[\frac{x_k y_k z_k^2}{x_k^2 + y_k^2}\right] + \mu_3\sigma_r^2(\lambda_2 - \lambda_3) E\left[\frac{x_k y_k z_k^2}{r_k^2(x_k^2+y_k^2)}\right] \\
&\quad + \left[(\lambda_2 - \lambda_3)\mu_2 - \lambda_1^2\mu_1^2\right] E\left[\hat{x}_{k|k-1}\hat{y}_{k|k-1}\right]
\end{aligned}
$$

$$
\begin{aligned}
S_{13} &= \lambda_1(\mu_2 - \mu_3)\left\{P_{k|k-1}(1,3) + \sigma_r^2 E\left[\frac{x_k z_k}{r_k^2}\right]\right\} \\
&\quad + \left[(\mu_2 - \mu_3)\lambda_1 - \lambda_1^2\mu_1\right] E\left[\hat{x}_{k|k-1}\hat{z}_{k|k-1}\right] \\
S_{23} &= \lambda_1(\mu_2 - \mu_3)\left\{P_{k|k-1}(2,3) + \sigma_r^2 E\left[\frac{y_k z_k}{r_k^2}\right]\right\} \\
&\quad + \left[(\mu_2 - \mu_3)\lambda_1 - \lambda_1^2\mu_1)\right] E\left[\hat{y}_{k|k-1}\hat{z}_{k|k-1}\right]
\end{aligned}
$$

In actual application, as follows approximation:

$$
\begin{cases}
E\left[\hat{x}_{k|k-1}^2\right] \approx \hat{x}_{k|k-1}^2 \\
E\left[\hat{y}_{k|k-1}^2\right] \approx \hat{y}_{k|k-1}^2 \\
E\left[\hat{z}_{k|k-1}^2\right] \approx \hat{z}_{k|k-1}^2
\end{cases}
$$

$$
\begin{cases}
E\left[\hat{x}_{k|k-1}\hat{y}_{k|k-1}\right] \approx \hat{x}_{k|k-1}\hat{y}_{k|k-1} \\
E\left[\hat{x}_{k|k-1}\hat{z}_{k|k-1}\right] \approx \hat{x}_{k|k-1}\hat{z}_{k|k-1} \\
E\left[\hat{y}_{k|k-1}\hat{z}_{k|k-1}\right] \approx \hat{y}_{k|k-1}\hat{z}_{k|k-1}
\end{cases}
$$

$$
\begin{cases}
E\left[\dfrac{x_k^2}{r_k^2}\right] \approx \dfrac{\hat{x}_{k|k-1}^2}{\hat{x}_{k|k-1}^2 + \hat{y}_{k|k-1}^2 + \hat{z}_{k|k-1}^2} \\
E\left[\dfrac{y_k^2}{r_k^2}\right] \approx \dfrac{\hat{y}_{k|k-1}^2}{\hat{x}_{k|k-1}^2 + \hat{y}_{k|k-1}^2 + \hat{z}_{k|k-1}^2} \\
E\left[\dfrac{x_k^2}{r_k^2}\right] \approx \dfrac{\hat{z}_{k|k-1}^2}{\hat{x}_{k|k-1}^2 + \hat{y}_{k|k-1}^2 + \hat{z}_{k|k-1}^2} \\
E\left[\dfrac{x_k^2 + x_k^2}{r_k^2}\right] \approx \dfrac{\hat{x}_{k|k-1}^2 + \hat{y}_{k|k-1}^2}{\hat{x}_{k|k-1}^2 + \hat{y}_{k|k-1}^2 + \hat{z}_{k|k-1}^2}
\end{cases}
$$

$$
\begin{cases}
E\left[\dfrac{x_k y_k}{r_k^2}\right] \approx \dfrac{\hat{x}_{k|k-1}\hat{y}_{k|k-1}}{\hat{x}_{k|k-1}^2 + \hat{y}_{k|k-1}^2 + \hat{z}_{k|k-1}^2} \\
E\left[\dfrac{x_k z_k}{r_k^2}\right] \approx \dfrac{\hat{x}_{k|k-1}\hat{z}_{k|k-1}}{\hat{x}_{k|k-1}^2 + \hat{y}_{k|k-1}^2 + \hat{z}_{k|k-1}^2} \\
E\left[\dfrac{y_k z_k}{r_k^2}\right] \approx \dfrac{\hat{y}_{k|k-1}\hat{z}_{k|k-1}}{\hat{x}_{k|k-1}^2 + \hat{y}_{k|k-1}^2 + \hat{z}_{k|k-1}^2}
\end{cases}
$$

$$
\begin{cases}
E\left[\dfrac{x_k y_k z_k^2}{(x_k^2 + x_k^2)}\right] \approx \dfrac{\hat{x}_{k|k-1}\hat{y}_{k|k-1}\hat{z}_{k|k-1}^2}{(\hat{x}_{k|k-1}^2 + \hat{y}_{k|k-1}^2)} \\
E\left[\dfrac{x_k y_k z_k^2}{(x_k^2 + x_k^2) r_k^2}\right] \approx \dfrac{\hat{x}_{k|k-1}\hat{y}_{k|k-1}\hat{z}_{k|k-1}^2}{(\hat{x}_{k|k-1}^2 + \hat{y}_{k|k-1}^2)(\hat{x}_{k|k-1}^2 + \hat{y}_{k|k-1}^2 + \hat{z}_{k|k-1}^2)}
\end{cases}
$$

IMM-BLUE filtering algorithm for maneuvering target tracking can be deduced by replacing model filter in IMM algorithm with BLUE filtering.

3 Data fusion

Through angle info fusion of radar and ESM sensors and radial distance measured from radar, pseudo-observation information can be over-all combined and therefore able to accurately estimate target state[12]. Fig.1 shows the implementation of radar-ESM data fusion.

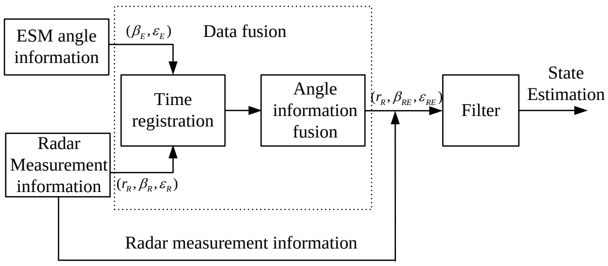

Fig.1. Flow chart of Radar- ESM data fusion

3.1 Time registration

General solution of time alignment is to collect all data to a sensor data with long scanning period[13, 14]. Usually, ESM data rate is higher that that of radar. This paper shows interpolation process of radar measured data. Suppose there are m measured values within one radar measurement period $[t_k, t_{k+1}]$, that is, $Z_E(k+j) = [\beta_E(k+j), \varepsilon_E(k+j)]^T$, $j = 1, \cdots, m-1$, while Δt_j is time difference between $Z_E(k+j)$ and radar value $Z_R(k) = [r_R(k), \beta_R(k), \varepsilon_R(k)]^T$ at time k. According to interpolation and extrapolation, time alignment equation for radar and ESM is:

$$
\tilde{Z}_R(t_e) = Z_R(t_1) + \frac{Z_R(t_2) - Z_R(t_1)}{t_2 - t_1}(t_e - t_1) \tag{25}
$$

The responding variance is:

$$\tilde{\sigma}_R^2 = \sigma_R^2 \cdot \left[1 + 2\left(\frac{\Delta t_j}{t_2 - t_1} \right)^2 \right] \tag{26}$$

Therein, t_e is observation time of ESM, t_1 and t_2 are adjacent observation times of radar, while $t_1 \le t_e \le t_2$, $\Delta t_j = t_e - t_1$, $\sigma_R^2 = \begin{bmatrix} \sigma_{Rr}^2 & \sigma_{R\beta}^2 & \sigma_{R\varepsilon}^2 \end{bmatrix}^T$. $\tilde{Z}_R(t_e) = \begin{bmatrix} \tilde{r}_R(t_e) & \tilde{\beta}_R(t_e) & \tilde{\varepsilon}_R(t_e) \end{bmatrix}^T$ is pseudo measurement value at time t_e after radar time alignment, $\tilde{\sigma}_R^2 = \begin{bmatrix} \tilde{\sigma}_{\tilde{r}_R}^2 & \tilde{\sigma}_{\tilde{\beta}_R}^2 & \tilde{\sigma}_{\tilde{\varepsilon}_R}^2 \end{bmatrix}$ is the pseudo variance value after radar time alignment.

3.2 Track fusion

Upon temporal registration of radar and ESM measurement, it is ready for angle fusion. This paper makes data fusion through weighted variance. Take azimuth for example, correlative radar trace point $\tilde{\beta}_R$ and ESM trace point β_E, target azimuth after data fusion is:

$$\beta_F = \sigma_\beta^2 \left(\frac{\tilde{\beta}_R}{\tilde{\sigma}_{\tilde{\beta}_R}^2} + \frac{\beta_E}{\sigma_{\beta_E}^2} \right) \tag{27}$$

Azimuth variance of fusion target is:

$$\sigma_\beta^2 = \frac{\tilde{\sigma}_{\tilde{\beta}_R}^2 \cdot \sigma_{E\beta}^2}{\tilde{\sigma}_{\tilde{\beta}_R}^2 + \sigma_{E\varepsilon}^2} \tag{28}$$

Similarly, the same fusion process can be applied for pitching angle from radar to ESM, then combined with distance info $\tilde{r}_R$ observed by radar at the corresponding time and target observation info is $(r_F, \beta_F, \varepsilon_F)$ after fusion. Accurate target positioning and tracking can be realized by filtering algorithm.

4 Target tracking in DBZ

The Doppler shift expression of the target radiation source is[15]:

$$f_{dt} = \frac{f_0}{c} v_r = \frac{f_0}{c} \left[\frac{(\dot{x} - \dot{x}_p)(x - x_p) + (\dot{y} - \dot{y}_p)(y - y_p) + (\dot{z} - \dot{z}_p)(z - z_p)}{\sqrt{(x - x_p)^2 + (y - y_p)^2 + (z - z_p)^2}} \right] \tag{29}$$

Where, v_r is radial velocity of target against sensor and stays positive when it points to target. f_0 is emission frequency of target radiation source, c is the propagation velocity of target emitter signal. $\dot{x}$, $\dot{y}$, $\dot{z}$ are relatively components of target velocity vector in X-velocity, Y-velocity and Z-velocity while $\dot{x}_p$, $\dot{y}_p$, $\dot{z}_p$ are components of aerial carrier velocity vector in X, Y and Z.

Radar is unable to detect targets when they drop in DBZ and begin to lose target track provided that DBZ is equivalent to $|f_{dt}| \le \Delta f$ and equivalent speed threshold is $[-L_0, L_0]$.

4.1 Data fitting in DBZ

Target when dropping into DBZ will be tracked by data fusion method combing IMM-BLUE based airborne radar and ESM. Target in an assumed DBZ which is not wide enough will continue former movement until it flies out of DBZ. During the period that target stays in DBZ, target distance information can be simulated by target estimate state from radar-ESM data fusion. This data fitting estimate can be approximately regarded as measured value of complete information. Generally, a time polynomial is able to fit target movement track. Suppose target moving track in X, Y and Z directions can be fitted as:

$$\begin{cases} \hat{x}_e(k) = a_0 + a_1 k + \cdots + a_m k^m \\ \hat{y}_e(k) = b_0 + b_1 k + \cdots + b_m k^m \\ \hat{z}_e(k) = z_0 + z_1 k + \cdots + z_m k^m \end{cases} \tag{30}$$

From the above, a_i, b_i, z_i ($i = 0,1,2,\cdots m$) are undetermined coefficients, while m is the polynomial order. This paper applies three-order polynomial to build motion model based on the target location by curve-fitting estimation.

Fig.2 presents the structure diagram of tracking algorithm combing radar and ESM in DBZ. Take data fitting value as the measured value z_k of IMM-BLUE and update the state estimation.

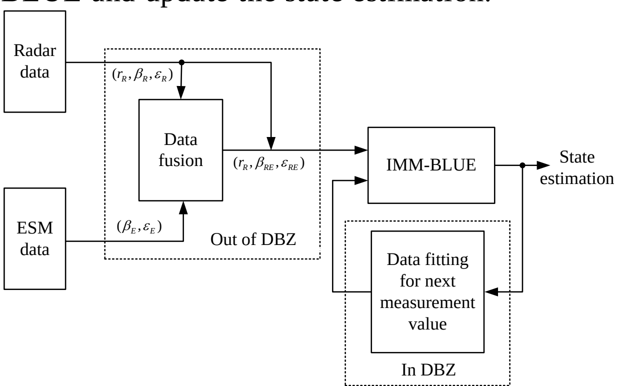

Fig.2. Structure diagram of tracking algorithm combing radar and ESM in DBZ

4.2 Only ESM tracking in DBZ

ESM is a passive sensor with azimuth angle and pitch angle as measurement data only, unable for target tracking normally, but with a known initial position, target tracking can be done through EKF filtering method with angles info only[16, 17, 18, 19]. Design structure diagram for the whole tracking algorithm is shown in Fig.3. When target drops into an assumed narrow DBZ, radar is unable to detect the target but only ESM measured data. Taking the predicted value $\hat{x}_{k|k}$ of radar-ESM fusion tracking estimated value at time k of last step, as the initial value of single ESM tracking at time $k+1$, tracking can be done by IMM-EKF filtering method.

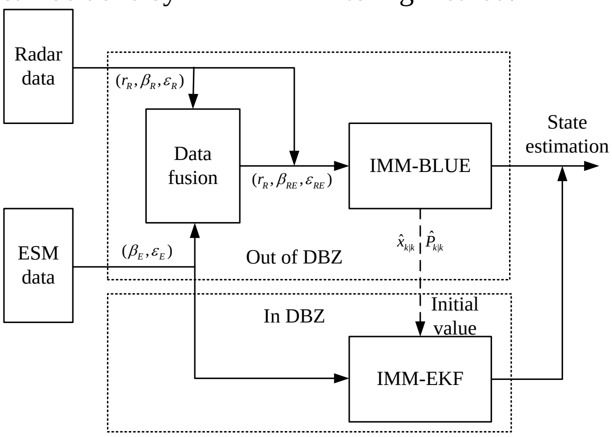

Fig.3. Structure diagram of only ESM tracking in DBZ

5 Simulation results and analysis

5.1 Target tracking algorithm

The parameters of target are given as follows. The sampling rate of radar and ESM is t=0.1s. The initial conditions of the target is (100000m, 50000m, 10000m) for position and (-230m/s, -230m/s, -40m/s) for velocity. The segments are defined as follows. 1st segment, t= (0-10)s, constant velocity flight with acceleration 0. 2nd segment, t= (10-85) s, 'S' type acceleration maneuver, 3rd segment, t= (85-100) s, constant velocity flight with acceleration 0. The initial conditions of the aircraft is (40000m, 20000m, 5000m) for position and (300m/s, 250m/s, 0m/s) for velocity. The segments are defined as follows. 1st segment, t= (0-20) s at angular speed of $\omega=2$ moving to the left. 2nd segment, t= (20-40) s moving at angular speed of $\omega=3$ to the left. 3rd segment, t= (40-60) s moving at angular speed $\omega=1$ to the right. 4th segment, t= (60-80) s moving at angular speed $\omega=2$ to the right. 5th segment, t= (80-100) s moving at angular speed $\omega=3$ to the right. Measurement noise covariance of radar radial distance, azimuth angle and pitch angle are $\sigma_R=50^2$, $\sigma_{R\beta}=(\pi/360)^2$, $\sigma_{R\varepsilon}=(\pi/360)^2$. Measurement noise covariance of ESM azimuth angle and pitch angle are $\sigma_{E\beta}=(\pi/300)^2$, $\sigma_{E\varepsilon}=(\pi/300)^2$ [20]. The model transition probability and original model probability are: $P=\begin{bmatrix}0.99 & 0.01\\ 0.01 & 0.99\end{bmatrix}$, $\mu=[0.5 \quad 0.5]$. Performance evaluation of maneuvering target is made separately by IMM-EKF and IMM-BLUE. Position error in directions of X, Y and Z are shown in Fig 4, 5 and 6. Table 1 is RMSE comparison of state estimation through IMM-EKF and IMM-BLUE filters. Seen from simulation results, IMM-EKF algorithm discards easily with worse tracking accuracy which is mainly caused by EKF algorithm error to linearization of non-linear measuring equations while IMM-BLUE shows better stability and tracking accuracy comparatively.

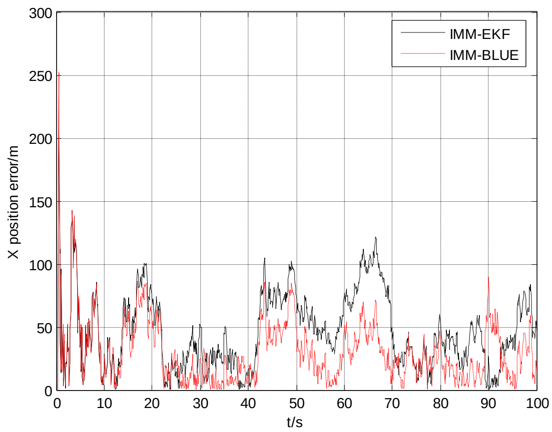

Fig.4. Position error comparisons in X direction

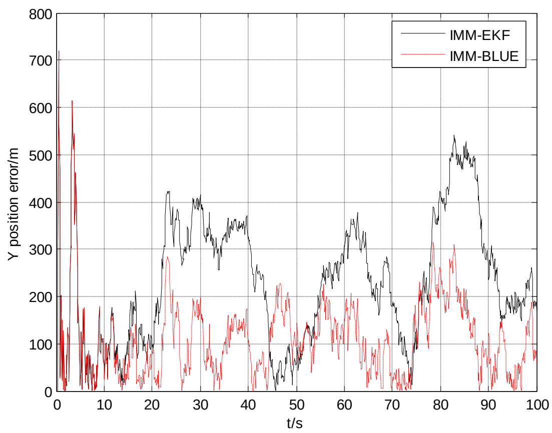

Fig.5. Position error comparisons in Y direction

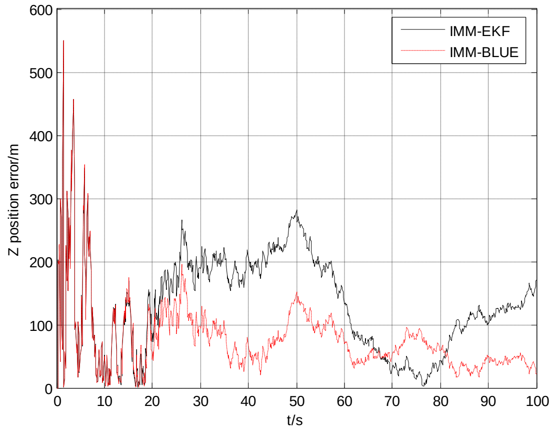

Fig.6. Position error comparisons in Z direction

Table 1 Comparison of state estimation RMSE

	X/m	Y/m	Z/m
IMM-EKF	130.11	165.69	152.77
IMM-BLUE	69.87	89.43	100.05

5.2 Radar and ESM fusion tracking

This paper applies IMM-BLUE tracking algorithm and makes simulated analysis on both radar measured value and fusion data. The detailed simulation results are shown in the following figures, among which Fig.7, Fig.8 and Fig.9 respectively stands for position error in X, Y and Z direction. Table 2 is mean square error comparison between single radar tracking and fusion tracking of radar and ESM. Seen from simulation results, target tracking accuracy of radar-ESM data fusion is higher than that of single radar tracking. Data fusion tracking algorithm for airborne radar based on IMM-BLUE and ESM contributes a lot to improve positioning and tracking accuracy.

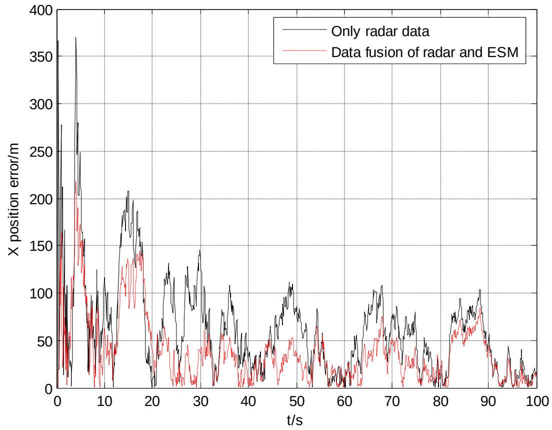

Fig.7. Position error comparisons in X direction

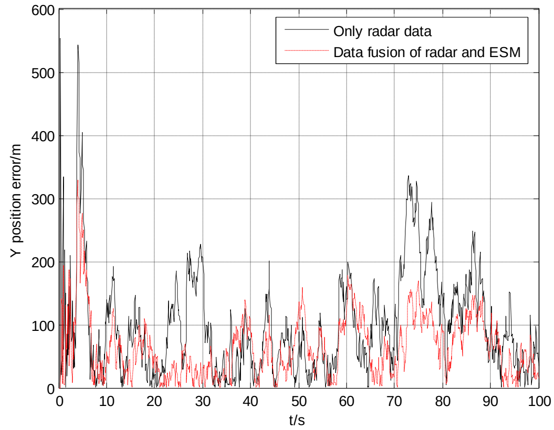

Fig.8. Position error comparisons in Y direction

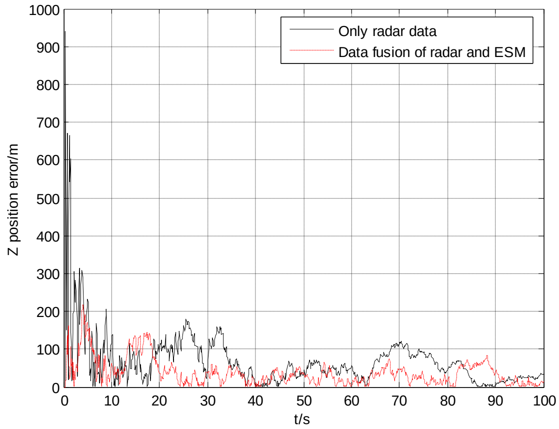

Fig.9. Position error comparisons in Z direction

Table 2 Comparison of state estimation RMSE

	X/m	Y/m	Z/m
Radar tracking	130.11	165.69	152.77
Fusion tracking	69.87	89.43	100.05

5.3 Target tracking in BDZ

Suppose the emission frequency of target radiation source is $f_0 = 1.2$ GHZ, and speed limit of DBZ target is $L_0 = 50$ m/s. Learn by formula (29), DBZ target section is [–200 200] HZ. Fig.10 shows the changing status of Doppler frequency and while two sections of target motion trail are within DBZ.

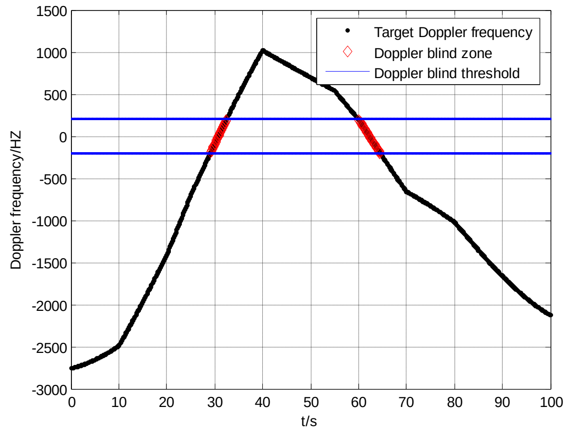

Fig.10. Doppler frequency

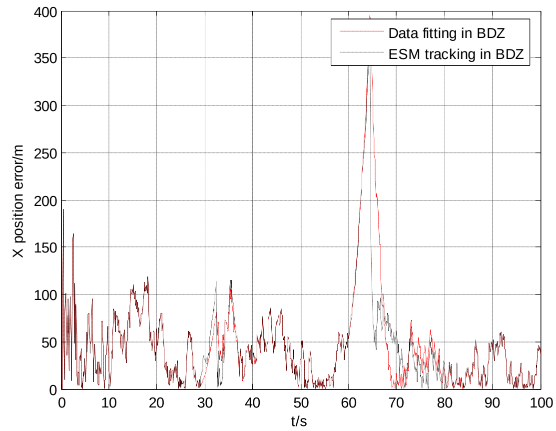

Fig.11. Position error comparisons in X direction

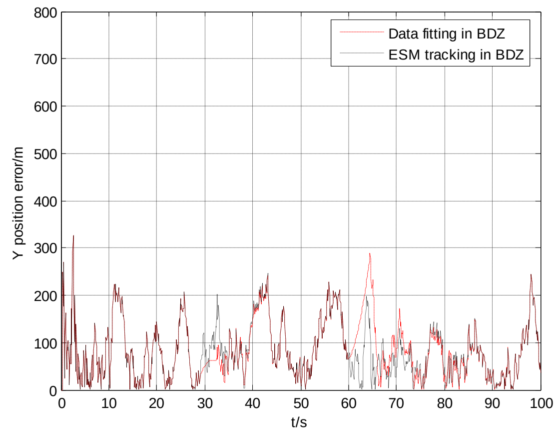

Fig.12. Position error comparisons in Y direction

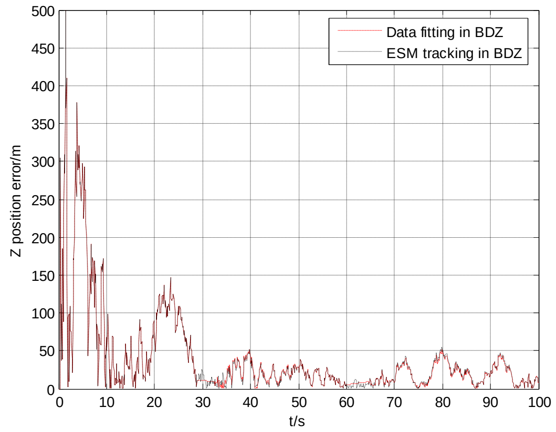

Fig.13. Position error comparisons in Z direction

Fig.11, Fig.12 and Fig.13 separately shows position error curve of X direction, Y direction and Z direction in DBZ, seen from which curve fitting method and single ESM tracking can both perform well, proving the validity of the two maneuvering target tracking methods for DBZ in this paper.

6 Conclusion

This paper presents maneuvering target tracking algorithm for airborne radar and based on which, it completes maneuvering target tracking by aerial radar-EMS data fusion through IMM-BLUE algorithm and designs the tracking method for targets in DBZ, proposing target tracking methods respectively for data fitting value in DBZ and single ESM tracking. Simulation results show IMM-BLUE algorithm not only overcomes the defect of EKF algorithm easy to diverge but enjoys a better tracking effect. Application of radar-ESM data fusion has further improved target tracking accuracy. Curve fitting and single ESM tracking can both achieve good target tracking effects in DBZ. Radar-ESM joint tracking technology in this paper has solved the problems caused by sensor unicity and Doppler blind zone.

References:

[1] LI W, Leung H, ZHOU Yifeng. Space time registration of radar and ESM using unscented Kalman filter[J]. *IEEE Transactions on Aerospace and Electronic Systems*, Vol.40, No.3, 2004,pp. 824-836.

[2] ZHOU Yifeng, MICKEAL J. A sequential ESM track association algorithm based on the use of information theoretic criteria[C]. *2007,*

10th International Conference on Information Fusion. Ottawa, Canada, 2007, pp. :1-7.

[3] U An-ping, JING Zhong-liang, HU Shi-qiang. UKF-based multi-sensor passive tracking with active assistance[J]. *Jourhal of Systems Engineering and Electronics,* Vol.17, No.2, 2006,pp. 245-250.

[4] Gordon N, Ristic B. Tracking airborne targets occasionally hidden in the blind Doppler[J]. *Digital Signal Processing,* Vol.12, No.2, 2002,pp. 383-393.

[5] Han Wei, Tang Zi-yue, Zhu Zhen-bo. Target tracking method using bearing information of ESM in Doppler blind zone[J]. *Systems Engineering and Electronics,* Vol.35, No.8, 2013,pp. 1650-1655.

[6] Han Wei, Tang Zi-yue, Zhu Zhen-bo. Method of target track optimization in Doppler blind zone[J]. Journal of Air Force Early Warning Academy, Vol.27, No.1, 2013,pp. 32-35.

[7] Kong A, Liu J S, Wong W H. Sequential imputations and bayesian missing data problems[J]. *Jounal of American Statistical Association,* Vol. 89, No. 425, 1994, pp.278-288.

[8] V. Vaidehi, K. Kalavidya, S. Indira Gandhi. Cluster-based centralized data fusion for tracking maneuvering targets using interacting multiple model algorithm[J]. *Sadhana,* Vol. 29, No. 2, 2004, pp.205-216.

[9] ROBERT A. SINGER. Estimating optimal tracking filter performance for manned maneuvering targets[J]. *IEEE Transactions on Aerospace and Electronic Systems,* Vol.6, No. 4, 1970, pp. 473-483.

[10] Pan-long Wu, Bao-bao Wang, Cun-hui Ji. Design and realization of short range defence radar target tracking system based on DSP/FPGA[J]. *WSEAS Transactions on System,* Vol. 10, No. 11, 2011, pp.376-386.

[11] Zhao Z L, Li X Rong, Jilkov V P. Best linear unbiased filtering with nonlinear measurements for target tracking[J]. *IEEE Transactions on Aerospace and Electronic Systems,* Vol.40, No.4, 2004,pp. 1324-1337.

[12] Anthony Spiteri Staines, Filippo Neri. A Matrix Transition Oriented Net for Modeling Distributed Complex Computer and Communication System[J]. *WSEAS Transactions on System,* Vol. 13, 2014, pp.12-22.

[13] Bao-shu Wang, Fang-she Li. The research on multiple targets tracking based on the data fusion technique[J]. *Journal of Xidian University,* Vol.25, No. 3, 1998, pp. 269-272.

[14] Michail Papoutsidakis, Dimitrios Pipomalis, Filippo Neri, Michel Camilleri. Intelligent Algorithms Based on Data Processing for Modular Robotic Vehicles Control[J]. *WSEAS Transactions on System,* Vol. 13, 2014, pp.242-251.

[15] Fang Li, Chen Xiangping, Zou Zhenwu. Research on Detection Blind Zones for Airborne PD Radar[J]. *Energy Procedia,* Vol. 13, 2011, pp.5630-5638.

[16] WU Pan-long, WANG Bao-bao, CAI ya-dong. Single observer passive target tracking based on extended H_∞ filter[J]. *Journal of Chinese Inertial Technology,* Vol. 18, No. 5, 2010, pp.591-594.

[17] Lian-zheng Zhang, Pan-long Wu, Xin-yu Zhang. Air defense missile detonation delay control Based on FPGA/DSP[J]. *WSEAS Transactions on System,* Vol. 12, No. 4, 2013, pp.202-211.

[18] WU Pan-long, CAI ya-dong, WANG Bao-bao. Satellite bearings-only tracking using extended Kalman particle filter[J]. *Infrared and Laser Engineering,* Vol. 40, No. 10, 2011, pp.2008-2013.

[19] WU Pan-long, CHEN Feng, WANG Bao-bao. Multi-station bearings-only maneuvering target passive tracking based on robust H_∞ filter [J]. *Systems Engineering and Electronics,* Vol. 33, No. 1, 2011, pp.17-20.

[20] Michel Camilleri, Filippo Neri, Michail Papoutsidakis. An Algorithmic Approach to Parameter Selection in Machine Learing using Meta-Optimization Techniques[J]. *WSEAS Transactions on System,* Vol. 13, 2014, pp.203-212.